Astron. Astrophys. 333, 1112–1116 (1998)

ASTRONOMY AND ASTROPHYSICS

Experimental cross section of ^{144}Sm$(\alpha,\gamma)^{148}$Gd and implications for the p-process

E. Somorjai[1], Zs. Fülöp[1], Á.Z. Kiss[1], C.E. Rolfs[2], H.P. Trautvetter[2], U. Greife[2], M. Junker[3], S. Goriely[4], M. Arnould[4], M. Rayet[4], T. Rauscher[5], and H. Oberhummer[6]

[1] ATOMKI, P.O. Box 51, H-4001 Debrecen, Hungary
[2] Ruhr-Universität, Universitätstrasse 150, D-44780 Bochum, Germany
[3] INFN LNGS, Assergi, L'Aquila, Italy
[4] Institut d'Astonomie et d'Astrophysique, C.P.226, Université Libre de Bruxelles, bd. du Triomphe, B-1050 Brüssel, Belgium
[5] Institut für theoretische Physik, Universität Basel, Klingelbergstrasse 82, CH-4056 Basel, Switzerland
[6] Institut für Kernphysik, Technische Universität Wien, Wiedner Hauptstrasse 8–10, A-1040 Wien, Austria

Received 20 October 1997 / Accepted 2 January 1998

Abstract. The cross section of the ^{144}Sm$(\alpha,\gamma)^{148}$Gd reaction has been measured at bombarding energies in the 10.5-13.4 MeV range using an activation method based on the off-line α-activity measurement of the ^{148}Gd residual nucleus. The long measuring time of the α-decay has required the use of etched track detectors. The resulting cross sections and astrophysical S-factors are compared to new statistical model calculations. The measured data at low energies reflect the strong energy dependence of the optical potential which is found to affect significantly our predictions of the α-capture rate.

Key words: nuclear reactions, nucleosynthesis, abundances – supernovae: general – solar system: general

1. Introduction

The stable neutron-deficient isotopes of the elements with charge number $Z \geq 34$ are classically referred to as the p-nuclei. They have been observed in the solar system only, where they represent 0.1% to 1% of the bulk amount of the more neutron-rich s- and r-isotopes.

The stellar mechanism synthesizing the p-nuclei is referred to as the p-process. It is generally agreed today that it develops in the O-Ne-rich layers of Type II supernovae as the result of the transformation of pre-existing s- or r-nuclides by photodisintegrations of the (γ,n), (γ,p) or (γ,α) type, possibly complemented with some neutron captures (Rayet et al. 1995). The modelling of the p-process requires the computation of an extended reaction network involving nuclei in the 12≤A≤210 mass range. Above Si, all the reaction rates are calculated with the help of a statistical model of the Hauser-Feshbach type. Experimental data are indeed very scarce in that mass region. In particular, Fülöp et al.(1996), Laird et al. (1987) and Verdieck & Miller (1967) provide measured sub-Coulomb cross sections for charged particle captures by nuclei heavier than Fe.

A specific question of great interest that has a direct bearing on the p-process has recently been raised by the observational discovery of the signature of the in-situ decay of ^{146}Sm ($t_{1/2} \approx 10^8$ y) in meteorites. These studies infer a ratio $(^{146}\mathrm{Sm}/^{144}\mathrm{Sm})_0 = 0.008 \pm 0.001$ at the start of the sequence of condensation of solids in the solar system (subscript 0) (Harper 1996, and references therein). One could attempt building up a p-process chronometry on this value if the corresponding isotopic production ratio could be estimated reliably enough at the p-process site.

In fact, this production ratio is still largely uncertain, ranging from about 0.015 to 1.5 (Rayet et al. 1995; Woosley & Howard 1990; Clayton et al. 1993; Howard & Meyer 1993). These widely different predictions are due in part to differences in the envisioned astrophysical conditions, and in part to nuclear physics uncertainties, especially in the ^{148}Gd(γ,α)^{144}Sm to ^{148}Gd(γ,n)^{147}Gd branching ratio (Woosley et al. 1990; Rayet & Arnould 1992). The astrophysical rates for these reactions are classically evaluated from a Hauser-Feshbach model for the neutron and α-particle captures, complemented with the use of the detailed balance theorem in order to obtain the reverse photodisintegration rates. In this framework, the α-particle capture rates are especially uncertain, in particular as a result of the poor knowledge of the proper optical potential to be used at the energies of astrophysical relevance.

In order to put the predicted ^{146}Sm/^{144}Sm production ratio on a safer footing, an (α,α) elastic scattering experiment has been performed recently (Mohr et al. 1997) with the aim of better constraining the parameters of the α-^{144}Sm optical potential. The present paper reports on the continuation of this experimental effort (see also Somorjai et al. 1997), and more specifically on the direct measurement of the ^{144}Sm(α,γ)^{148}Gd cross section down to energies very close to the Gamow energy window ($E_{\mathrm{G}} \approx 9.5$ MeV) of relevance to the ^{144}Sm production.

Send offprint requests to: Zs. Fülöp

It is also shown that the obtained experimental data can be reproduced by a Hauser-Feshbach calculation with an α-nucleus optical potential satisfying several physical constraints.

Sect. 2 describes the experimental set-up used to measure the ^{144}Sm(α,γ)^{148}Gd cross section. The resulting data are compared with rate predictions in Sect. 3. The impact of the new Hauser-Feshbach rate that accounts for the experimental data on the ^{146}Sm/^{144}Sm production ratio predicted for Type II supernovae is analyzed in Sect. 4, where a brief conclusion is also drawn.

2. The experimental set-up

The experimental investigation of the $^{144}\mathrm{Sm}(\alpha,\gamma)^{148}\mathrm{Gd}$ reaction has been performed at the MGC cyclotron in Debrecen and at the Dynamitron Tandem accelerator in Bochum in the energy range E_α=10.5 to 13.4 MeV ($E_{\rm cm}$= 10.22-12.99 MeV). An average He^{++} target current of 1 particle-μA has been used to avoid target deterioration. The accumulated charge for the irradiation varied between 100 mC and 1 C, depending on the bombarding energy.

Since the cross section is determined via the off-line detection of the α-decay of the ^{148}Gd residual nuclei, the α-activity of the target material (as well as the backing) is not desirable. The well known reductive evaporation of Sm oxide (Westgaard & Bjørnholm 1966) proved to be unsuitable as a result of the small contamination by the α-activity of the lanthanum used for the reduction. In contrast, the electrophoresis method (Bjørnholm et al. 1959) provided samarium oxide targets free from disturbing α-activity. The thickness of the Sm oxide targets varied between 20 and 350 μg/cm^2. The ^{144}Sm oxide material was enriched to 87% and 96%[1] and deposited onto thin Al or Ni foils.

The prepared targets were analysed by RBS (Rutherford Backscattering) and PIXE (Proton Induced X-ray Emission). Fig. 1 shows the diffusion-like RBS pattern of the loose structure of the samarium oxide grains on the backing in comparison with the metallic Sm produced by reductive evaporation. To increase the target stability during the bombardment, a very thin aluminium layer was evaporated onto the samarium oxide layer.

A chamber containing a surface barrier detector for the detection of the scattered α-particles has been constructed for the irradiations. The yield of the scattered particles has been used to monitor the target stability during the irradiation process. An electric field of -300 V was applied to eliminate the effect of secondary electrons on the beam integration.

At low energies (long runs), the extracted cross section values have been occasionally corrected for slight target deterioration followed continuously by the monitor detector. The necessity of this kind of correction was additionally checked by RBS measurements before and after the long runs.

Poly-allyl-diglycol-carbonate (TASTRAK, England) etched track detectors have been used for the determination of

[1] obtained from CIL, USA and CAMPRO, The Netherlands, respectively

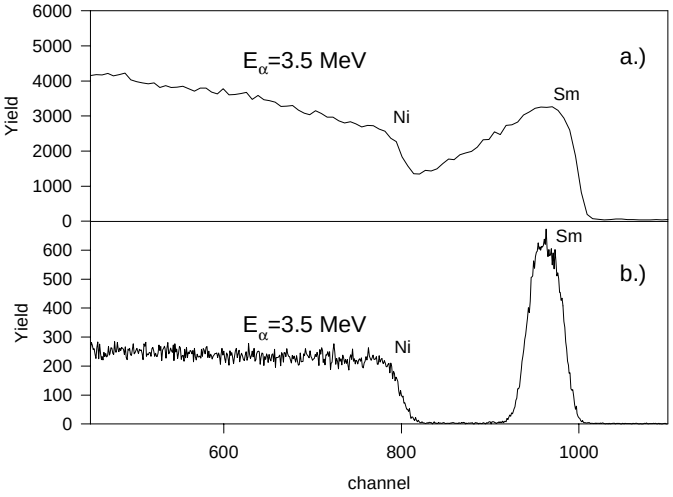

Fig. 1a and b. RBS spectra from (**a**) Sm oxide (beaded surface), and (**b**) metallic Sm targets on nickel backing

the number of α-particles emitted from the ^{148}Gd residual nuclei. Track detectors were exposed to the targets in 2π geometry in normal air conditions at room temperature. Exposure times varied between 2 weeks and half a year. Etching was performed in a 6.25N NaOH solution at 70°C for 3 hours. Track counting was done manually using an optical microscope. Separation of the 3.18 MeV α-particle tracks (^{148}Gd) from the 2 MeV ones (background) was done by track size and shape comparison on a visual basis. Detection efficiency of the track detector and of the track counting method was used to obtain the number of ^{148}Gd nuclei on the target.

The α-activity of non-irradiated, natural and enriched targets has also been measured to check the effect of contaminants. For confirmation of the experimental results, targets irradiated at the high end of the α-particle bombarding energy region have also been measured by surface barrier Si-detector (600 mm^2) in an underground laboratory having very low background (INFN, Gran Sasso, Italy). The α-particle spectra from a target before and after irradiation at E$_\alpha$= 13.355 MeV are shown in Fig. 2. The extracted activities agree excellently with the ones from track detectors.

3. Experimental results and model predictions

The derived cross sections and astrophysical S-factors are provided in Fig. 3 and in Table 1. They are obtained by adopting the value $t_{1/2}(^{148}\mathrm{Gd}) = 74.6 \pm 3$ y for the ^{148}Gd half-life (Prestwood et al. 1981; Peker 1990). Different values would be extracted with the use of the longer half-lives that can also be found in the literature (e.g. Friedman et al. 1966). The quoted experimental errors (10-45%) on the cross sections do not take these half-life uncertainties into account. They are in fact dominated by the target inhomogeneities monitored by RBS measurements of different spots on the targets.

These experimental data are compared with Hauser-Feshbach predictions. At the relatively low energies studied in the present experiment, the radiative α-capture cross sections

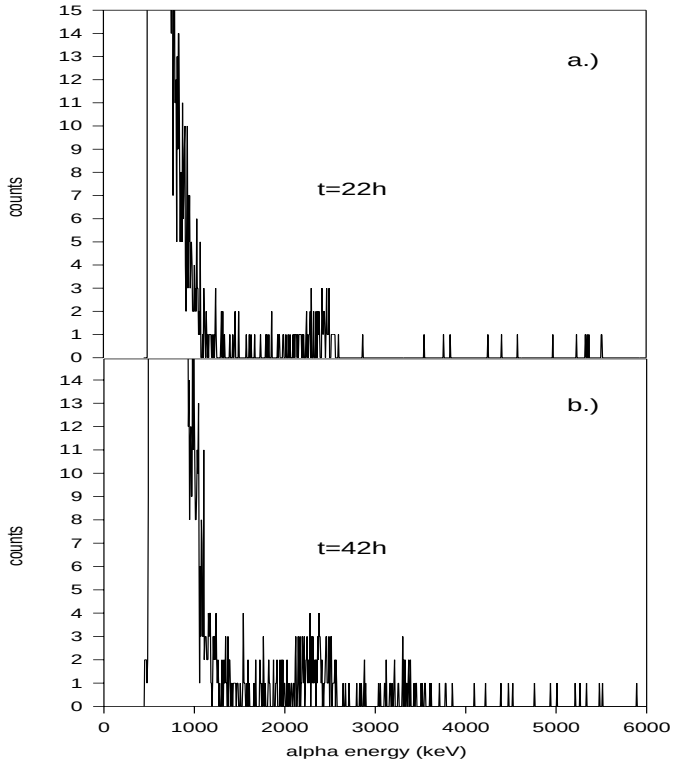

Fig. 2a and b. The α-particle spectra from a target (**a**) before and (**b**) after irradiation

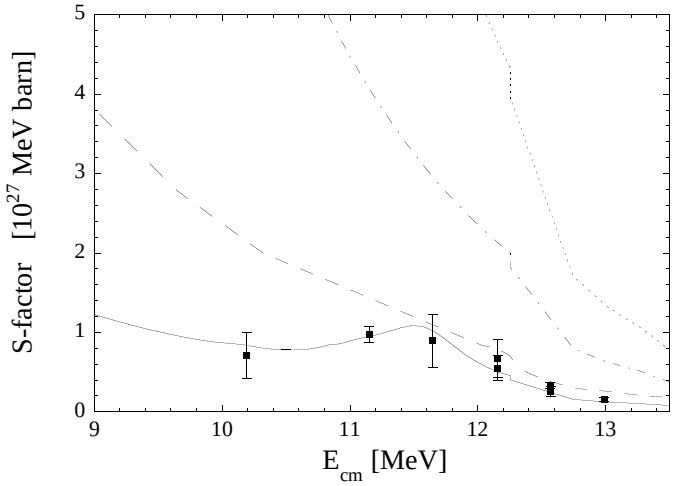

Fig. 3. The astrophysical S-factor for $^{144}\mathrm{Sm}(\alpha,\gamma)^{148}\mathrm{Gd}$. The dot-dash and dotted lines are estimates obtained with the Hauser-Feshbach code MOST and the global α-nucleus optical potentials of Mann (1978) (as used in the code SMOKER) and Avrigeanu et al. (1994), respectively. The solid line is obtained with the code MOST and the energy-dependent optical potential developed in this work. The dashed line is from Mohr et al. (1997)

are mainly sensitive to the α-particle transmission coefficient evaluated from an α-nucleus optical potential. There is little experimental information on such potentials, especially at the low sub-Coulomb energies of astrophysical relevance. This is why most of the proposed potentials are derived from fits to elastic

Table 1. Experimental cross sections and S-factors for ^{144}Sm(α,γ)^{148}Gd

E_α [a)]	$E_{\rm cm}^{\rm eff.}$ [b)]	σ	$\Delta\sigma$	$S(\Delta S)$
MeV	MeV	μbarn	μbarn	10^{26} MeV-barn
10.500	10.193	0.083	0.034	7.13 (2.92)
11.500	11.151	2.9	0.3	9.76 (1.01)
12.000	11.647	12.1	4.5	8.94 (3.32)
12.509	12.156	39.2	14.1	6.74 (2.42)
12.505	12.159	32.4	9.0	5.52 (1.53)
12.939	12.571	45.7	11.0	2.55 (0.61)
12.942	12.568	59.0	5.9	3.33 (0.33)
13.355	12.992	83.2	16.6	1.58 (0.31)

[a)] errors for $E_\alpha \leq 12$ MeV and for others are $\pm$ 1.5 keV and $\pm$ 7 keV (cyclotron), respectively
[b)] calculated from the target thicknesses

α-nucleus scattering data at energies $\gtrsim 80$ MeV (Nolte et al. 1987) or, in some cases, to (n,α) cross sections at lower energies (Avrigeanu et al. 1994). Two predictions using global potentials derived on such grounds (Mann 1978; Avrigeanu et al. 1994) and the Hauser-Feshbach code MOST[2] are displayed in Fig. 3. Quite clearly, the results obtained with the use of such potentials lead to cross section predictions that substantially disagree with experiment.

In order to improve the situation, Mohr et al. (1997) have constructed a potential constrained at low energy by a $^{144}\mathrm{Sm}+\alpha$ scattering experiment performed at $E_{\rm lab} = 20$ MeV. Fig. 3 shows that the corresponding S-factors are put in agreement with our experimental results at energies $E_{\rm cm} \gtrsim 11.5$ MeV, while a large discrepancy persists at lower energies. This results from the steady increase of the predicted S-factor with decreasing energies which strongly contrasts with the experimental data.

In fact, tests conducted with the code MOST demonstrate that this remarkable experimental energy trend of the S-factor can be accounted for by making use of a suitably chosen energy-dependent α-nucleus optical potential with a Woods-Saxon shape. More specifically, this potential is constructed on grounds of the following requirements:
(i) the volume integral of the imaginary part of the potential has to decrease with decreasing energies, as implied by elastic α-scattering experimental data (e.g. Atzrott et al. 1996). This is achieved by selecting an energy dependence of the depth of the imaginary potential of the form

$$W(E) = W_0 \left[1 + \exp\left(-\frac{E-E^*}{a^*}\right)\right]^{-1}, \qquad (1)$$

where the values of the free parameters W_0, E^* and a^* are selected in order to reproduce the available values of the volume

[2] MOST is a Hauser-Feshbach code developed by one of the authors (S. Goriely 1997) from the code SMOKER (Thielemann et al. 1986), with respect to which it features some new physical ingredients (esp. ground state description, level densities, GDR properties)

integral of the imaginary potential derived from experiments at $E_{\rm lab} = 20$ and 120 MeV;
(ii) the measured elastic scattering cross sections at $E_{\rm lab} = 20$ MeV reported by Mohr et al. (1997) and reaction cross sections presented here have to be reproduced at best by the calculations;
(iii) the values of the parameters of the real part of the optical potential have to be reasonably close to those that allow the reproduction of α-decay properties (Buck et al. 1993).

These combined constraints lead to the following selection of parameter values [in complement to the free parameters appearing in Eq. (1), classical notations are adopted for the Woods-Saxon shaped real (subscript v) and imaginary (subscript w) parts of the potential]: $V_0 = 162.3$ MeV, $r_v = 1.27$ fm, $a_v = 0.48$ fm, $W_0 = 19$ MeV, $r_w = 1.57$ fm, $a_w = 0.60$ fm, $E^* = 19$ MeV and $a^* = 2$ MeV. The resulting potential exhibits an energy dependence that is much stronger at low energies than the one given by Atzrott et al. (1996) and Mohr et al. (1997), even if the same experimental elastic scattering data at $E_{\rm lab} = 20$ and 120 MeV are reproduced in all cases. As demonstrated by Fig. 3, this new optical potential is able to account remarkably well for the cross section data of Fig. 3 and Table 1, including the $E \leq 11.5$ MeV experimental points.

Of course, the potential tailored here for the ^{144}Sm(α,γ)^{148}Gd case is not expected to have any global character. As an example, it leads to a substantial disagreement with the experimental cross sections for the reaction ^{70}Ge(α,γ)^{74}Se (Fülöp et al. 1996). In fact, a good fit to these data can be obtained by selecting the new values $E^* = 9$ MeV and $a^* = 2$ MeV in the above-mentioned potential. This most likely illustrates the widely expected mass and energy dependence of the sub-Coulomb α-nucleus optical potential. Still, this dependence remains largely unknown, and could be unravelled by more systematic scattering and reaction measurements below the Coulomb barrier.

The potential derived above predicts a Maxwellian-averaged rate of $1.3\,10^{-16}$cm^{3}s^{-1}mole^{-1} at $T = 2.5\,10^9$ K. This is about 10 and 6 times lower than the latest predictions of Rauscher et al. (1995) and of Mohr et al. (1997), respectively. By application of the detailed-balanced theorem, the rate of the reverse ^{148}Gd(γ,α)^{144}Sm reaction (denoted in the following by $\lambda_{\gamma\alpha}$) is reduced accordingly.

4. Astrophysical implications and conclusions

The revised value of $\lambda_{\gamma\alpha}$ is used to re-evaluate the production ratio $P \equiv {}^{146}{\rm Sm}/{}^{144}{\rm Sm}$ in the SNII models considered in Rayet et al. (1995). Its values are shown in Fig. 4 for stars with main sequence masses $M = 13$, 15, 20 and 25 $M_\odot$ and compared with the values obtained by using the old estimate for $\lambda_{\gamma\alpha}$ calculated with the global α-nucleus optical potentials of Mann (1978) (see Fig. 3). The revision of $\lambda_{\gamma\alpha}$ to smaller values lowers the production of ^{144}Sm, and favours concomitantly the ^{146}Sm synthesis through the main production channel ^{148}Gd(γ,n)^{147}Gd(γ,n)^{146}Gd (β^+)^{146}Sm. As a net result, the P values are increased.

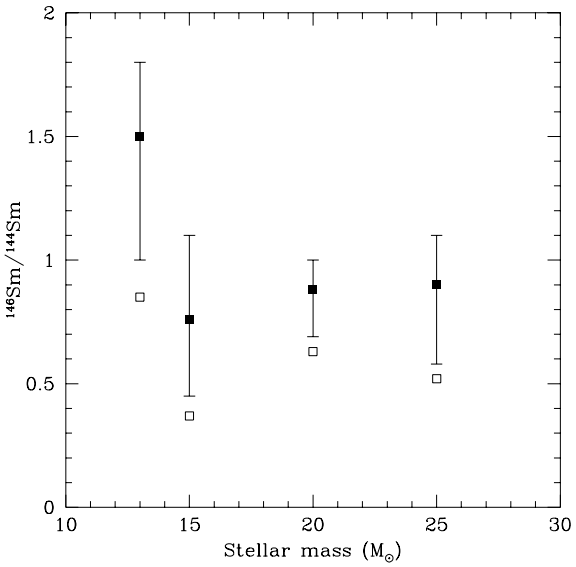

Fig. 4. The production ratio $P \equiv {}^{146}{\rm Sm}/{}^{144}{\rm Sm}$ in the explosion of stars with masses $M = 13$, 15, 20 and 25 $M_\odot$, calculated with 2 different rates for ^{148}Gd(γ,α)^{144}Sm. Open squares: using the global α-nucleus optical potential of Mann (1978). Full squares: using the energy-dependent optical potential developed in this work (see Fig. 3). The error bars show the effect on P of uncertainties in the rates for the (γ,α) and (γ,n) reactions on ^{148}Gd (see text)

Other nuclear problems add to the uncertainty in the evaluation of P. This concerns in particular the ^{148}Gd(γ,n) ^{147}Gd reaction, for which no experimental information can be foreseen in a very near future in view of the unstable nature of ^{147}Gd ($t_{1/2} \approx 38$ h). The present calculations of P use for the rate of that reaction, $\lambda_{\gamma{\rm n}}$, a theoretical value calculated with the Hauser-Feshbach code MOST. In order to estimate the dependence of P on $\lambda_{\gamma\alpha}$ and $\lambda_{\gamma{\rm n}}$, we vary $\lambda_{\gamma\alpha}$ by a factor 3 and $\lambda_{\gamma{\rm n}}$ by a factor 2. So doing, we consider to span reasonable ranges of uncertainty. The upper and lower bounds obtained for P assuming these variations correspond to the combinations ($\lambda_{\gamma\alpha}/3\,,\ \lambda_{\gamma{\rm n}} \times 2$) and ($\lambda_{\gamma\alpha} \times 3\,, \lambda_{\gamma{\rm n}}/2$), respectively. Those bounds are shown as error bars in Fig. 4. It is seen that the values of P obtained in SNII explosions of stars of different masses are definitely increased with the new value of $\lambda_{\gamma\alpha}$ determined in this work, although the effect of uncertainties on $\lambda_{\gamma\alpha}$ and $\lambda_{\gamma{\rm n}}$ remains important.

In addition, astrophysical uncertainties concur to the difficulty of predicting P reliably. The pre-supernova structure and, correlatively, the characteristics of the shock at the supernova stage may depend on uncertain nuclear quantities like e.g. the ^{12}C(α,γ)^{16}O rate. We find that the value $P = 0.90$ obtained for a 25 $M_\odot$ star (Fig. 4) is increased to 2.1 when we use a SNII model calculated with a smaller (by a factor ≈ 2.3) ^{12}C(α,γ)^{16}O rate (see Rayet et al. (1995) for a short discussion of this rate and of its effect on the p-process yields). Another problem concerns the possible contribution of Type Ia supernovae (SNIa) to the production of the p-nuclei, and in particular of the Sm proton-rich isotopes. In a preliminary calculation using the de-

flagration model W7 of Nomoto et al. (1984) [3], we find $P = 1$, in agreement with the values we obtain for SNII models. In contrast, Howard and Meyer (1993) predict a very small value ($P = 0.04$) with the delayed detonation model of Khokhlov (1991). This large difference can hardly be attributed to nuclear physics uncertainties alone, and should partly result from differences in the considered SNIa simulations. The latter are still very uncertain, so that any conclusion on the contribution of SNIa events to the samarium problem is premature.

Limiting ourselves to the ^{144,146}Sm production in SNII events, we conclude that the small value of the ^{148}Gd(γ,α)^{144}Sm rate resulting from the present experiment brings the ^{146}Sm/^{144}Sm production ratios in the range $0.7 < P < 2$, and discards values smaller than 0.5. These values have to be compared with the ratio $(^{146}\mathrm{Sm}/^{144}\mathrm{Sm})_0 \simeq 0.008$ prevailing in the solar system when solids started to form (see Introduction). Here we restrict this confrontation to the following simplistic astrophysical scenario: one or several SNII explosions are responsible for a "late" ^{144}Sm and ^{146}Sm contamination of the solar system which already contains ^{144}Sm originating from the general galactic nucleosynthesis. Let us (i) call Δ^* the time delay between these supernova events and the start of the condensation of solids, (ii) assume that the late contamination is thoroughly mixed with the rest of the solar system material, and (iii) introduce a "dilution" factor d, the inverse of which is a measure of the efficiency of the late contamination, or in other words, the fraction of the lately produced ^{144}Sm and ^{146}Sm that finds its way into forming solids. If $\Delta^* \ll t_{1/2}(^{146}\mathrm{Sm}) \approx 10^8$ y, and if $0.5 \lesssim P \lesssim 2$, the considered late SNII events can account for $(^{146}\mathrm{Sm}/^{144}\mathrm{Sm})_0 \simeq 0.008$ if $6\,10^3 \lesssim d \lesssim 2\,10^4$. This dilution is high enough for having some astrophysical plausibility, even if a careful discussion of the contaminating efficiency remains to be conducted in order to draw firmer conclusions. We just note here that the efficiency derived from the d values reported above may just represent an upper limit of the actual efficiency. Indeed, some events that have taken place at times commensurable with $t_{1/2}(^{146}\mathrm{Sm})$ might well have contributed to the solar ^{146}Sm. On the other hand, the late Sm contamination might not have been thoroughly mixed with the rest of the solar system material. Finally we remark that, from a study of the production of ^{107}Pd and other *short-lived* ($10^5 \lesssim t_{1/2} \lesssim 10^8$ y) radio-nuclides by Wolf-Rayet stars, Arnould et al (1997) obtain dilution factors (normalized on ^{107}Pd) in the range 3-4 10^3 for solar metallicity stars of mass between 40 and 85 $M_\odot$. The similarity of these results with our predictions, especially for our lowest values of P, is interesting considering that a WR star of 40 $M_\odot$ could well produce, in its supernova stage, proton-rich Sm isotopes in proportions similar to the ones obtained for lower mass stars, as suggested by Fig. 4.

Acknowledgements. This work was supported by PECO (Contract ERBCIPDCT94-0629), OTKA (No. T016638, W015608 and CW015604), the Hungarian-German and the Hungarian-Austrian exchange program (OMFB No. B123 and B43). We want to thank the LUNA Collaboration for the possibility of some measurements in LNGS, Gran Sasso, Italy. T.R. acknowledges support by an APART fellowship of the Austrian Academy of Sciences. S.G. is FNRS Senior Research Assistant and M.R. is FNRS Research Associate.

[3] We are indebted to M. Hashimoto for providing us with the temperature and density profiles of model W7 relevant to the p-process

References

Arnould M., Paulus G., Maynet G., 1997, A&A 321, 452
Atzrott U., Mohr P., Abele H., Hillenmayer C., Staudt G., 1996, Phys. Rev. C53, 1336
Avrigeanu V., Hodgson P.E., Avrigeanu M., 1994, Phys. Rev. C49, 2136
Bjørnholm S., Dam Ph., Nordby H., Roy Poulsen N.O., 1959, Nucl. Instr. Meth. 5, 196
Buck B., Merchant A.C., Perez S.M., 1993, At. Data Nucl. Data Tables 54, 53
Clayton D.D., Hartmann D.H., Leising M.D., 1993, ApJ Lett. 315, 25
Friedman A.M., Milsted J., Metta D. et al., 1966, Rad. Chem. Act. 5, 192
Fülöp Zs., Kiss Á.Z., Somorjai E. et al., 1996, Z.Phys. A355, 203
Goriely S., 1997, in: Proceedings of Nuclear Data for Science and Technology, Trieste (Italy), in press
Harper C.L., 1996, ApJ 466, 437
Howard W.M., Meyer B.S., 1993, in: Nuclei in the Cosmos, eds. F. Käppeler, K. Wisshak, IOP, Bristol, p.575
Khokhlov, A.M., 1991, A&A 245, 114
Laird C.E., Flynn D., Hershberger L.R., Gabbard F., 1987, Phys. Rev. C35, 1265
Mann F.M., 1978, Hauser 5, A Computer Code to Calculate Nuclear Cross Sections, Hanford Engineering HEDL-TME 78-83
Mohr P., Rauscher T., Oberhummer H. et al., 1997, Phys. Rev. C55, 1523
Nolte M., Machner H., Bojowald J., 1987, Phys. Rev. C36, 1312
Nomoto K., Thielemann F.-K., Yokoi K., 1984, ApJ 286, 644
Peker L.K., 1990, Nucl. Data Sheets 59, 393
Prestwood R.J., Curtis D.B., Cappis J.H., 1981, Phys. Rev. C24, 1346
Rauscher T., Thielemann F.K., Oberhummer H., 1995, ApJ Lett. 451, 37
Rayet M., Arnould M., 1992, in: Second International Conference on Radioactive Nuclear Beams, ed. Th. Delbar, IOP, Bristol, p. 347
Rayet M., Arnould M., Hashimoto M., Prantzos N., Nomoto K., 1995, A&A 298, 517
Somorjai E., Fülöp Zs., Kiss Á.Z. et al., 1997, Nucl. Phys. A621, 293c
Thielemann F.-K., Arnould M., Truran J.W., 1986, in: Advances in Nuclear Astrophysics, eds. E. Vangioni-Flam, J. Audouze, M. Cassé, J.-P. Chièze & J. Tran Thanh Van, Editions Frontières, Gif-sur-Yvette, p. 525
Verdieck E.V., Miller J.M., 1967, Phys. Rev. 153, 1253
Westgaard L., Bjørnholm S., 1966, Nucl. Instr. Meth. 42, 77
Woosley S.E., Howard W.M., 1990, ApJ Lett. 354, 21